Age-Related Differences in White Matter Integrity in Healthy Human Brain: Evidence from Structural MRI and Diffusion Tensor Imaging

Rishu Rathee*, V.P. Subramanyam Rallabandi* and Prasun K. Roy

Computational Neuroscience and Neuroimaging Division, National Brain Research Center, Manesar, Gurgaon, Haryana, India.
*These authors contriburted equally to this work.

ABSTRACT: The aim is to investigate the relationship between microstructural white matter (WM) diffusivity indices and macrostructural WM volume (WMV) among healthy individuals (20–85 years). Whole-brain diffusion measures were calculated from diffusion tensor imaging using FMRIB software library while WMV was estimated through voxel-based morphometry, and voxel-based analysis was carried out using tract-based spatial statistics. Our results revealed that mean diffusivity, axial diffusivity, and radial diffusivity had shown good correlation with WMV but not for fractional anisotropy (FA). Voxel-wise tract-based spatial statistics analysis for FA showed a significant decrease in four regions for middle-aged group compared to young-aged group, in 22 regions for old-aged group compared to middle-aged group, and in 26 regions for old-aged group compared to young-aged group ($P < 0.05$). We found significantly lower WMV, FA, and mean diffusivity values in females than males and inverted-U trend for FA in males. We conclude differential age- and gender-related changes for structural WMV and WM diffusion indices.

KEYWORDS: diffusion tensor imaging, white matter integrity, fractional anisotropy, mean diffusivity, radial diffusivity, axial diffusivity, tract-based spatial statistics

CITATION: Rathee et al. Age-Related Differences in White Matter Integrity in Healthy Human Brain: Evidence from Structural MRI and Diffusion Tensor Imaging. *Magnetic Resonance Insights* 2016:9 9–20 doi:10.4137/MRI.S39666.

TYPE: Original Research

RECEIVED: March 14, 2016. **RESUBMITTED:** April 19, 2016. **ACCEPTED FOR PUBLICATION:** April 26, 2016.

ACADEMIC EDITOR: Sendhil Velan, Editor in Chief

PEER REVIEW: Four peer reviewers contributed to the peer review report. Reviewers' reports totaled 1,622 words, excluding any confidential comments to the academic editor.

FUNDING: The research is supported by the Office of Principal Scientific Adviser (NKN), the Perception Engineering scheme, Dept. of Information Technology, Govt. of India, and the Tata Innovation Program, Dept. of Biotechnology, Govt. of India. The authors confirm that the funders had no influence over the study design, content of the article, or selection of this journal.

COMPETING INTERESTS: Authors disclose no potential conflicts of interest.

COPYRIGHT: © the authors, publisher and licensee Libertas Academica Limited. This is an open-access article distributed under the terms of the Creative Commons CC-BY-NC 3.0 License.

CORRESPONDENCE: pkroy@nbrc.ac.in

Paper subject to independent expert single-blind peer review. All editorial decisions made by independent academic editor. Upon submission manuscript was subject to anti-plagiarism scanning. Prior to publication all authors have given signed confirmation of agreement to article publication and compliance with all applicable ethical and legal requirements, including the accuracy of author and contributor information, disclosure of competing interests and funding sources, compliance with ethical requirements relating to human and animal study participants, and compliance with any copyright requirements of third parties. This journal is a member of the Committee on Publication Ethics (COPE).

Published by Libertas Academica. Learn more about this journal.

Introduction

Normal aging in the human brain manifests itself through structural and functional changes accompanied by cognitive decline even in the absence of disease. There have been several studies attempting to comprehend the age-related microstructural changes[1,2] and macrostructural degeneration of brain tissue.[3,4] White matter (WM) being an important factor in brain aging consists mostly of myelinated long distance axonal projections of neurons and glial cells, such as oligodendrocytes and astrocytes, which may be differently affected with age in mammals.[5] Some reports showed age-related changes in WM volume (WMV) along with different WM integrity indices[6] but specific relationship between micro- and macrostructural mechanisms remains unclear. Hence, it is important to study the relationship between the macrostructural measure, ie, WMV, derived from structural T1-weighted magnetic resonance imaging and the microstructural measures of WM integrity indices, such as fractional anisotropy (FA), mean diffusivity (MD), axial diffusivity (AD), and radial diffusivity (RD), using diffusion tensor imaging (DTI) to get an insight into life-span aging.

The atrophy of human WM with aging is caused by a loss of myelinated fibers with a small diameter.[7] Postmortem studies revealed progressive decrease in myelin lipid concentration starting from as early as 20–100 years of age.[8] Also, during normal aging, the myelin breakdown processes make a significant contribution to the degradation of cognitive processing speed.[9–11] On the other hand, water diffusion in WM tissue is stronger when parallel, rather than perpendicular to myelinated nerve fibers; DTI can be utilized to gain information about the integrity of nerve fibers. Thus, many features of WM are not directly related to myelin and may affect FA and WMV in different ways. Therefore, FA reflects aspects of axonal integrity and organization that are not related to myelin,[12] and myelin is not necessary for fibers to have significant diffusion anisotropy.[13] In addition to FA, AD and RD were also related to age and WMV.

Several investigations have been done on the age-related alterations in various measures of WM integrity. The effects of age and gender are not uniform with normal aging in several WM regions.[14] Age differences are found greatest for the parietal and occipital regions.[15] Evidence from early brain morphology studies has revealed greater total WMV in males than females.[16,17] The global effects of aging on brain volume, MD, and FA using voxel-based analysis showed that brain volume and FA were negatively correlated predominantly in anterior

structures and MD was positively correlated in the periventricular WM. These results indicate that diffusion properties and brain volume are complementary markers to the effects of aging.[18] The patterns of age-related differences in WM integrity measures, such as FA, AD, and RD, revealed a relatively new pattern (radial increase/axial decrease) that varied by brain region and may reflect differential aging of microstructural (eg, degree of myelination) and macrostructural (eg, coherence of fiber orientation) properties of WM.[19] The age-related changes, sex differences, and age-by-sex interactions in WM integrity (FA, AD, and RD) across the whole brain showed that global FA was negatively correlated with age and AD and RD were positively correlated with age.[20] Recent study reported linear and curvilinear correlations of FA, MD, and WMV with age in children.[21] Correlations between FA and age as well as between MD and age showed exponential trajectories in most regions of interest in males and females, except for several fibers, such as the corpus callosum connecting the bilateral rectal gyri in males.[21]

Earlier investigations also reported regional changes in MD and FA in the central nervous system during normal aging, and results showed a significant increase in MD in frontal WM and lentiform nucleus and significant FA decline in the genu of the corpus callosum with advancing age.[22] The regional basis of age-related alterations in prefrontal WM was noticed using DTI, and the results revealed that much of prefrontal WM showed a reduced FA with increasing age and obtained a significant correlation between prefrontal WM anisotropy and prefrontal WMV for the participants aged over 40 years. Thus, regionally accelerated alterations in prefrontal WM with aging illustrated FA's potential as a microstructural index of volumetric measures.[23,24] Another study showed the regional reduction in FA with aging in the whole brain. The results revealed that cerebral hemisphere, hippocampus, frontal lobe, corona radiata, corpus callosum, and internal capsule have decreased FA, and there was a strong negative correlation between age and FA in frontal lobe, hippocampus, and cerebral hemisphere, whereas there was a weaker negative correlation between corona radiate, corpus callosum, and internal capsule.[25]

The characterization of WM structural changes at the tract level, tract group (limbic, commissural, association, and projection tracts) level, and comprehensive analysis was done with four metrics (FA, MD, AD, and RD) derived from DTI.[26] The changes in FA were mapped for 11 major cerebral WM tracts; pointing tracts that reach their peak FA values later in life also showed progressively higher age-related decline than earlier maturing motor and sensory tracts.[27] In healthy aging, the trajectories of FA of cerebral WM and thickness of cortical gray matter have been reported as quadratic with age, but the relationship between them was found linear, indicating that a putative biological mechanism may explain the nonlinearity of their age trajectories.[28]

Although there are studies focused on WM diffusivity in healthy children, young aged (<40 years), older adults (>60 years), none of the studies reported the relationship between WMV and WM integrity indices. Also there are some concerns about methodological limitations, such as image resolution in DTI acquisition and DTI software or statistical discrepancies in estimating diffusion indices due to unequal number of subjects in each age group and gender. Nonetheless, it is necessary to understand relationship between the WM diffusivity indices and structural WMV in healthy aging specifically during the transition state from young-to-middle age or middle-to-old age. To overcome these limitations in existing studies, we aim to study the relationship between WM diffusion indices and WMV among three age groups (young, middle, and old) along with voxel-wise analysis of FA, MD, AD, and RD values calculated using tract-based spatial statistics (TBSS) and global WMV estimated from voxel-based morphometry (VBM).

Subjects and Methods

Dataset. Data used in performing this research were obtained from the Information eXtraction from Images (IXI) dataset (http://www.brain-development.org/). The dataset includes 600 MR images from normal, healthy subjects with no previous history of neurological dysfunction and a normal neurological examination. The data have been collected from three different hospitals in London, such as Hammersmith Hospital, Guy's Hospital, and Institute of Psychiatry. The data have been collected as a part of the project "IXI-Information eXtraction from Images (EPSRC GR/S21533/02)." This article involves the T1-weighted MR images and DT images (15 directions) from the dataset. In order to circumvent the issues of interscanner variability, we included images of Hammersmith Hospital only. There were a total of 181 participants from Hammersmith Hospital aged between 20 and 85 years, but we excluded a small number of subjects (n = 4) because of the availability of T1-weighted MR images of these subjects in contrast to the unavailability of DT images of these subjects in database. A total of 177 subjects (88 males and 89 females) aged 20–85 years with T1-weighted magnetic resonance images and DT images were included. Demographic information of participants is summarized in Table 1.

Table 1. Summary of demographic information of the subjects.

AGE GROUPS (YEARS)	COUNT (MALE/FEMALE)	MEAN ± SD (MALE/FEMALE)
20–40 (Young)	69 (43/26)	29.6 ± 5.61 (30.5 ± 5.96/28.1 ± 4.73)
41–60 (Middle)	52 (26/26)	50.2 ± 6.23 (51.2 ± 5.8/49.2 ± 6.5)
61–85 (Old)	56 (19/37)	67.2 ± 5.16 (68.3 ± 5.3/66.5 ± 5.05)

Image acquisition. T1-weighted magnetization prepared rapid acquisition gradient echo sequence and DTI scans were acquired using Philips Intera 3T scanner. Acquisition parameters for T1-weighted MRI scans were as follows: TR/TE = 9.6/4.6 ms, number of phase encoding steps = 208, echo train length = 208 ms, reconstruction diameter = 240 cm, acquisition matrix = 208 × 208, and flip angle = 8°. Single-shot echo-planar diffusion images comprised 15 diffusion-weighted volumes with gradient encoding applied in 15 noncollinear directions (b = 1000 s/mm^2) and 1 nondiffusion-weighted reference image (b_0 = 0 s/mm^2 with TR/TE = 11,894.4/51 ms, number of phase encoding steps = 110, reconstruction diameter = 224 cm, imaging matrix = 128 × 128, field of view = 224 × 224, in-plane resolution = 1.75 × 1.75 mm^2, slice thickness = 2 mm, acquisition matrix = 112 × 110, sense factor = 2, flip angle = 90°, and number of averages = 2).

Image processing. The processing pipeline was divided into two levels: T1-weighted MR image processing (using VBM) and DT image processing (using FMRIB software library [FSL]) as shown in Figure 1. VBM was performed on high-resolution T1-weighted structural images for tissue segmentation[29] using Statistical Parametric Mapping (SPM8)[30] software implemented in MATLAB 2010. Initially, T1-weighted MR images of subjects were segmented in native space into different tissue types, such as WM (c1), gray matter (c2), and cerebrospinal fluid (c3). Later a built-in SPM function (SPM_get_volume) was executed to acquire global WMV. The normalization of WMV was done by correction of intracranial volume.

DTI analyses. DTI data were processed using FSL.[31] Initially, DT images (15 direction) obtained for each subject were merged to form a single four-dimensional DT image, which was corrected for head movement and eddy current distortions using FDT's (FMRIB's Diffusion Toolbox) Eddy correct. The eddy-corrected image was then passed through the FSL Brain Extraction Tool to extract the brain and exclude skull, scalp, and other nonbrain tissues. The output of Brain Extraction Tool generated a binary brain mask, which was further used as an input file for the next step, ie, DTIFIT. Finally, DTIFIT was used to fit diffusion tensor model at each voxel, with the brain mask limiting the fitting of tensors to brain space. The output of DTIFIT yielded voxel-wise maps' eigenvalues

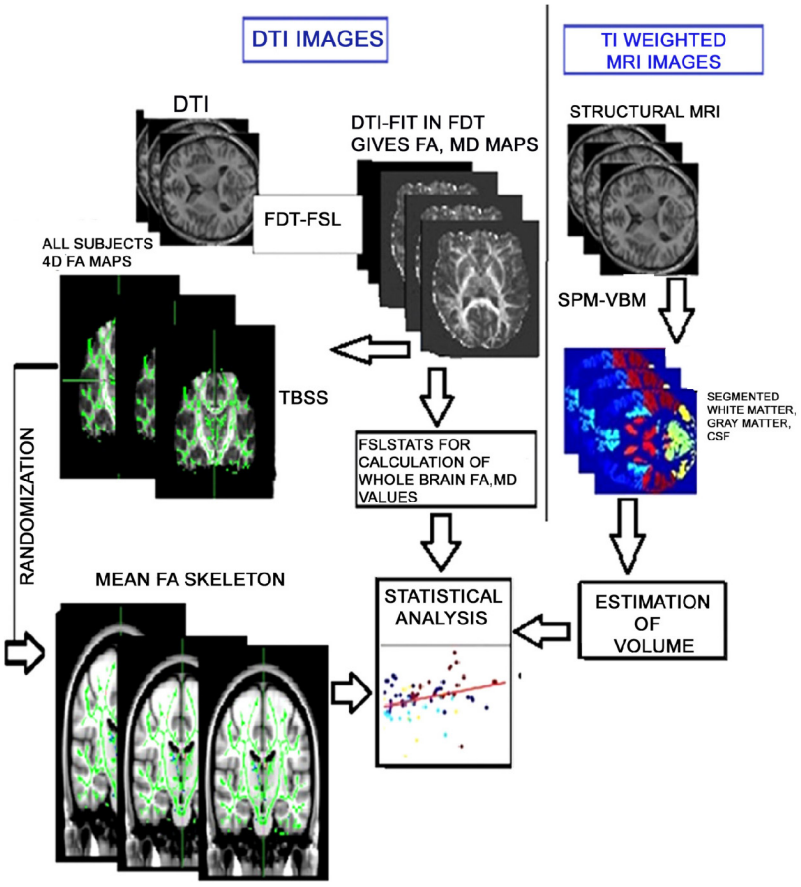

Figure 1. Processing pipeline depicting our methodology. Right: T1-weighted MR images undergo segmentation (white matter, gray matter, and CSF) and volumetric calculation through SPM and VBM followed by statistical analysis. Left: Diffusion indices (FA, MD, RD, and AD) are extracted from DTI images through FDT toolbox followed by volumetric calculation. On the other side, diffusion maps are subjected to TBSS for voxel-wise statistical analysis.
Abbreviations: CSF, cerebrospinal fluid; SPM, statistical parametric mapping; VBM, voxel-based morphometry; FA, fractional anisotropy; MD, mean diffusivity; RD, radial diffusivity; AD, axial diffusivity; TBSS, tract-based spatial statistics.

(L1, L2, and L3), FA, AD (L1), RD (average of L2 and L3), and MD. The threshold value of 0.2 is used in FSL stats for computing FA in single subject to see the prominent tracts.

Tract-based spatial statistics. Voxel-wise statistical analysis of diffusion indices was carried out in TBSS[32] implemented in FSL. In TBSS, between-group skeleton-wise statistical analysis was performed for diffusion indices. Initially, FA image of each subject undergo nonlinear registration to a standard FMRIB58_FA template followed by affine transformation into MNI152 1 mm^3 standard space resulting in a transformation of the original FA image into MNI152 space. All these are merged into a single four-dimensional image of all FA, and the mean of all FA images gives mean FA image. This mean FA image was used to generate a WM skeleton that identifies the center of WM tracts shared by all subjects. Mean FA skeleton was threshold to 0.2 to include the major WM pathways but exclude intersubject variability regions and partial volume effects. Each subject's prealigned FA image was registered to the mean FA skeleton, and then resulting skeletonized FA data undergo voxel-wise statistics that includes comparisons of FA among three age groups. This between-group test uses randomized tool to see significance at each voxel against a null distribution generated from 5000 random permutations of group membership. The significant WM clusters were identified with reference to the atlas tool JHU ICBM-DTI-81 WM labels. Later, other diffusion indices underwent TBSS using the FA images to achieve the nonlinear registration and skeletonization stages. Also, FA images are used to estimate the projection vectors from each individual subject onto the mean FA skeleton.

Statistical analysis. Age-related and gender-related statistical analysis for WMV and all the four diffusion indices was estimated between groups using nonpaired parametric group analysis of variance (ANOVA) with post-hoc pair-wise Bonferroni correction. Graphical representation of above analysis includes box plots in which boxes represent the lower and upper quartiles (blue solid lines) and the median measurement (red line) for each group. Whiskers indicate the sample minimum and maximum, whereas the represented outliers (dots) differ from the lower and upper quartiles by more than 1.5 times the interquartile range. For gender-related differences, the intergroup and within-group differences were represented by column graphs, and statistical analysis was performed using ANOVA. The correlation analysis between WMV and different diffusion indices is performed, and statistical analysis for regression is done using linear model.

Results

Age-related trends for various WM diffusivity indices. The results of age-related changes along with the whole-brain values of FA, MD, AD, and RD are shown in Figure 2. Box plot analysis indicates that the global WMV followed a similar trend of volume decline across an age range of 20–85 years. FA showed decline with age among the three age groups. Also MD, AD, and RD showed the same increasing pattern with age. In younger and middle age groups, the mean value remains in same range, whereas in old age group, there is an inflate increase in values of MD, AD, and RD.

The ANOVA results of the between groups for age and age and sex interaction-related trends for cerebral WM integrity indices are summarized in Table 2. Measures revealed that in young- vs middle-aged adults, there were no statistically significant differences for the values of global WMV, FA, MD, AD, and RD. However, there were statistically significant differences in middle- vs old-aged adults for global WMV, FA, MD, AD, and RD ($P < 0.05$). Moreover, in young- vs old-aged adults, there were statistically significant differences in the values of WMV, FA, MD, and AD ($P < 0.05$), but there were no significant differences for RD.

Gender differences. The overall gender differences for WMV and diffusion indices are shown in Figure 3. The analysis revealed that the global WMV, FA, and MD ($P < 0.05$) was significantly lower in female subjects than in male subjects and found no significant difference for AD and RD.

The gender-based within-group and intergroup differences are summarized in Figure 4. In young adults, the global values of AD and MD ($P < 0.05$) were significantly higher in males than in females, whereas the global values of WMV, FA, and RD exhibited no significant differences in male and female subjects. In middle-aged adults, the global values of WMV, MD, and AD ($P < 0.05$) were significantly higher in males than in females, whereas the global values of FA and RD show no significant differences in male and female subjects. In old-aged adults, the global values of WMV and AD ($P < 0.05$) were significantly higher in males than in females, whereas the global values of FA, MD, and RD showed no significant differences in male and female subjects.

The intergroup differences for male subject's WMV and diffusion indices measures revealed that in young- vs middle-aged adults, no statistically significant differences were found for the global values of WMV, FA, MD, AD, and RD. However, there were statistically significant differences in middle- vs old-aged adults for the global values of WMV and RD ($P < 0.05$). Moreover, in young- vs old-aged adults, there were statistically significant differences in the values of WMV ($P < 0.05$), FA, MD, and RD ($P < 0.05$). Altogether, for male subjects, we noticed a gradual decline in WMV, the quadratic trend (inverted-U) for FA values, and a gradual increase in the values of MD, AD, and RD ($P < 0.05$) across three age groups.

Measures revealed that in young- vs middle-aged adults, statistically significant differences were found in the global values of WMV ($P < 0.05$) and FA ($P < 0.05$). However, in middle- vs old-aged adults, there were statistically significant differences for RD ($P < 0.05$). Moreover, in young- vs old-aged adults, there were statistically significant differences in the WMV, MD, and RD ($P < 0.05$). Overall, for female subjects, we noticed a gradual decline in WMV and FA values,

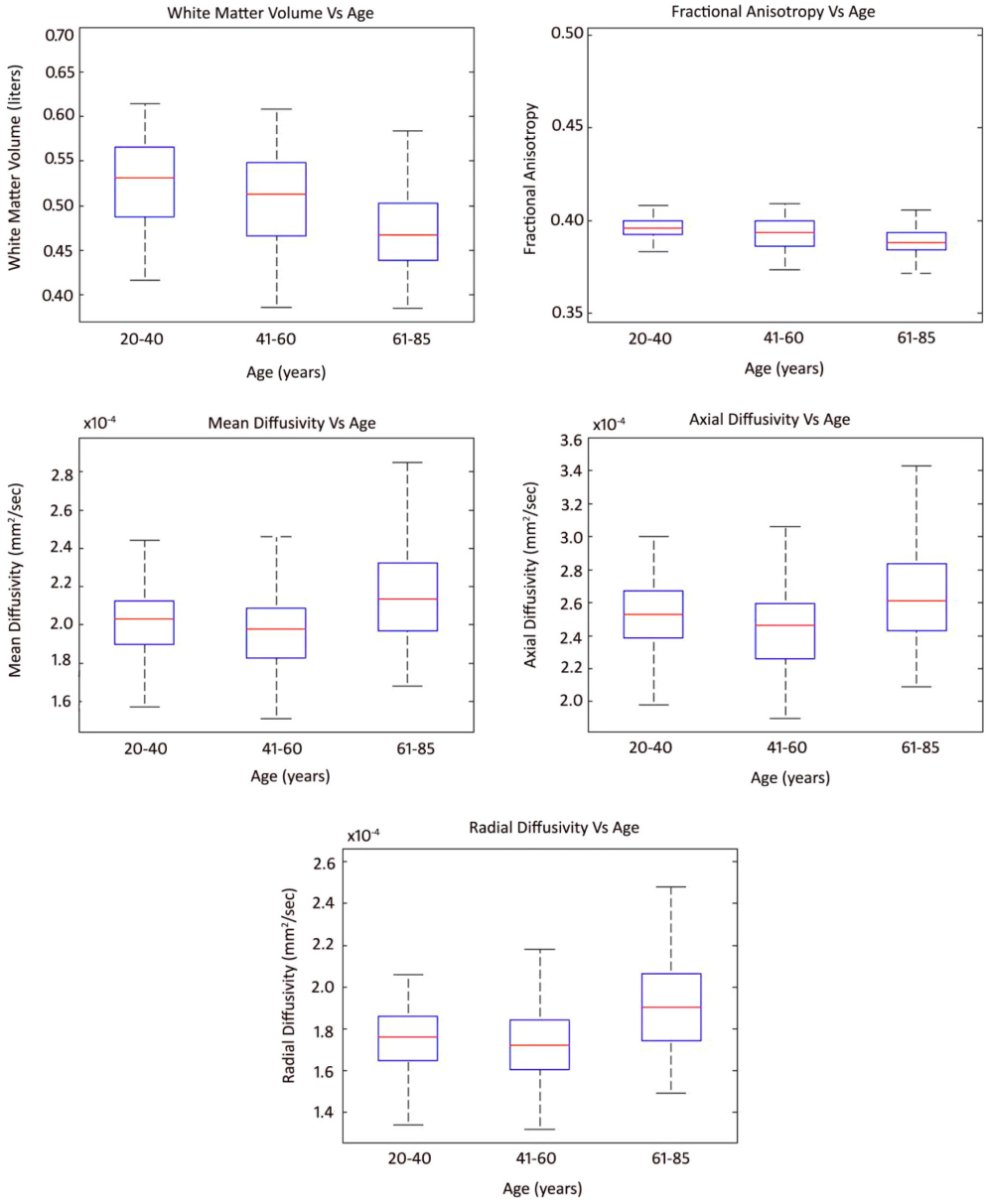

Figure 2. Box plots of whole-brain white matter volume, fractional anisotropy, mean diffusivity, radial diffusivity, and axial diffusivity in three age groups.

Table 2. ANOVA of age and sex interactions of various WM indices.

AGE AND SEX INTERACTION (BETWEEN GROUPS)	SS	df	MS	F	*P*-VALUE	F CRITICAL
White matter volume	0.181131	5	0.036226	15.0999	2.82E-12	2.266984
Fractional anisotropy	0.004343	5	0.000869	4.158908	0.001	2.266984
Mean diffusivity	2.98E-08	5	5.96E-09	12.5604	2.15E-10	2.266984
Axial diffusivity	4.01E-08	5	8.03E-09	11.72934	9.35E-10	2.266984
Radial diffusivity	2.59E-08	5	5.71E-09	13.32543	5.71E-11	2.266984
Age interaction						
White matter volume	0.068832	2	0.034416	11.46	0.00002	3.047096
Fractional anisotropy	0.002530	2	0.00127	5.890493	0.003	3.047096
Mean diffusivity	1.021E-08	2	5.1E-09	8.820833	0.0002	3.047096
Axial diffusivity	7.79E-09	2	3.9E-09	4.53604	0.01	3.047096
Radial diffusivity	1.18E-08	2	5.92E-09	12.8176	0.000006	3.047096

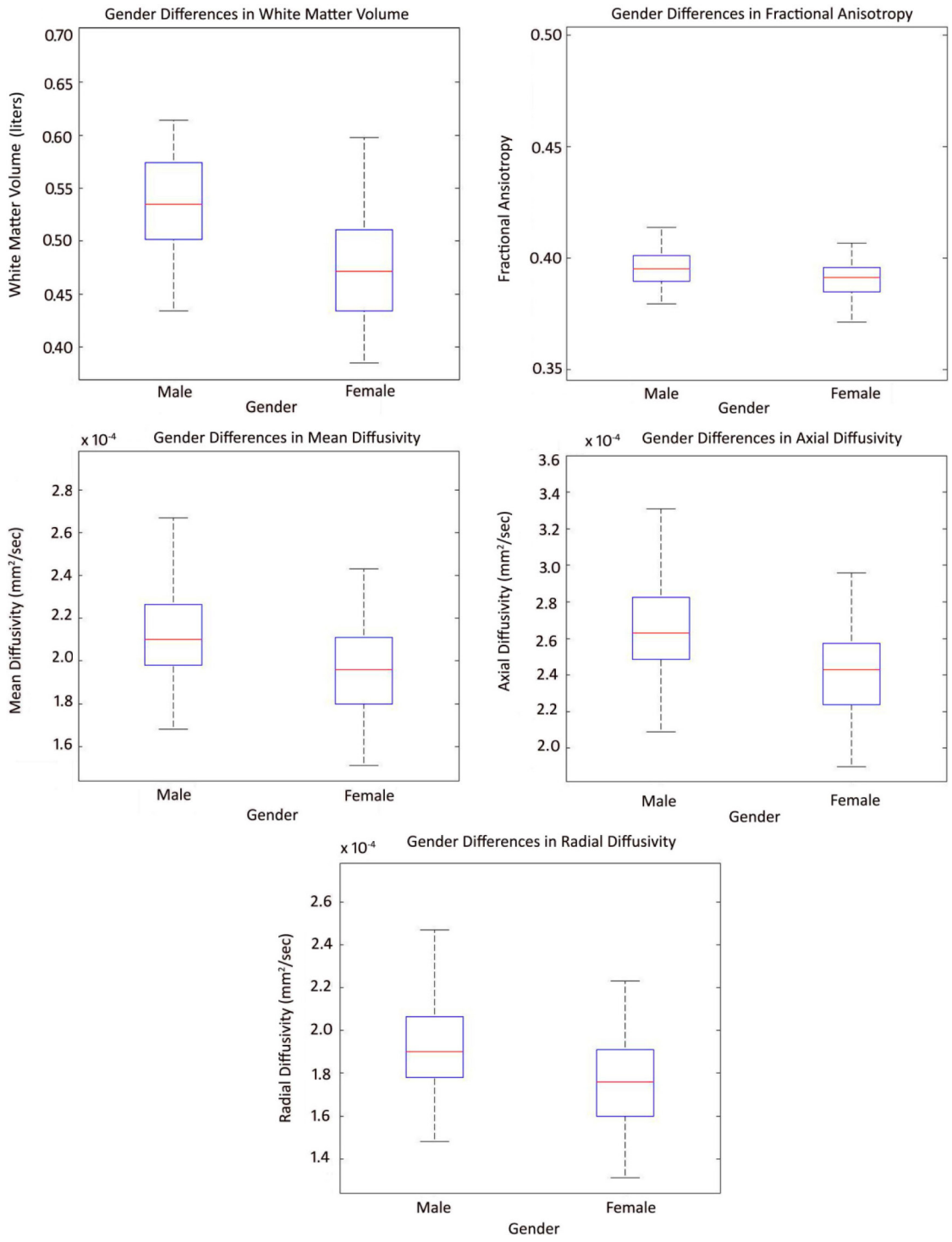

Figure 3. Box plots showing overall gender differences with whole-brain white matter volume, fractional anisotropy, mean, radial, and axial diffusivities.

and a gradual increase in the values of MD, AD, and RD ($P < 0.05$) across three age groups.

Intergroup voxel-wise statistics of FA. The between-group voxel-wise analysis revealed a significant decrease in FA in certain regions based on the TBSS voxel-wise statistics represented by color magnets superimposed on the mean FA skeleton in red–yellow color as shown in Figure 5, and MNI coordinates are summarized in Table 3.

TBSS analysis showed an increase in FA (young > middle) in four regions, including superior corona radiata R, superior corona radiata L, body of corpus callosum, and genus of corpus callosum ($P < 0.05$). In middle > old, we identified increased FA values in 22 regions of both left and right hemispheres ($P < 0.05$), namely superior corona radiata, body of corpus callosum, fornix, superior longitudinal fasciculus, anterior corona radiata, external capsule, posterior limb of

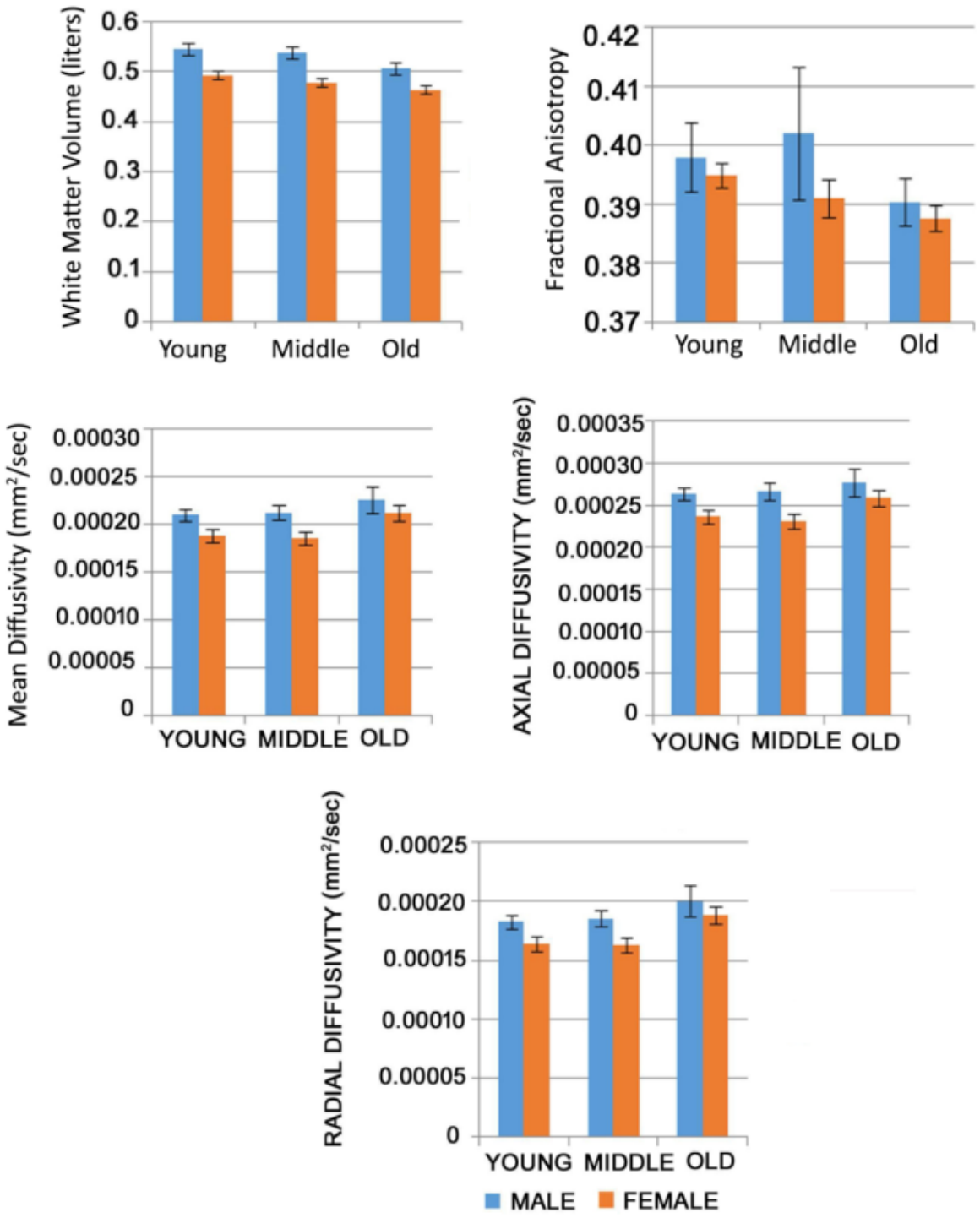

Figure 4. Column graphs showing within-group gender differences and intergroup differences of male and female with whole-brain white matter volume and each diffusion index. The standard errors are shown with black band above the columns.
Abbreviations: FA, fractional anisotropy; MD, mean diffusivity; AD, axial diffusivity; RD, radial diffusivity; WMV, white matter volume.

internal capsule, sagittal stratum including inferior frontooccipital fasciculus, cerebral peduncle, corticospinal peduncle, and middle cerebellar peduncle. Also in old > young, lower FA values were observed in 26 regions of both left and right hemispheres ($P < 0.05$), namely corpus callosum, cingulum, superior longitudinal fasciculus, anterior and posterior limb of internal capsule, anterior and superior corona radiata, sagittal striatum, external capsule, cerebral peduncle, fornix (stria terminalis), posterior thalamic radiation including optic radiation, and retrolentricular part of internal capsule. Also no regions of higher FA values in older than young-aged group were found.

However, we notice some regions, such as genu of corpus callosum, external capsule, and fornix, showed increase values

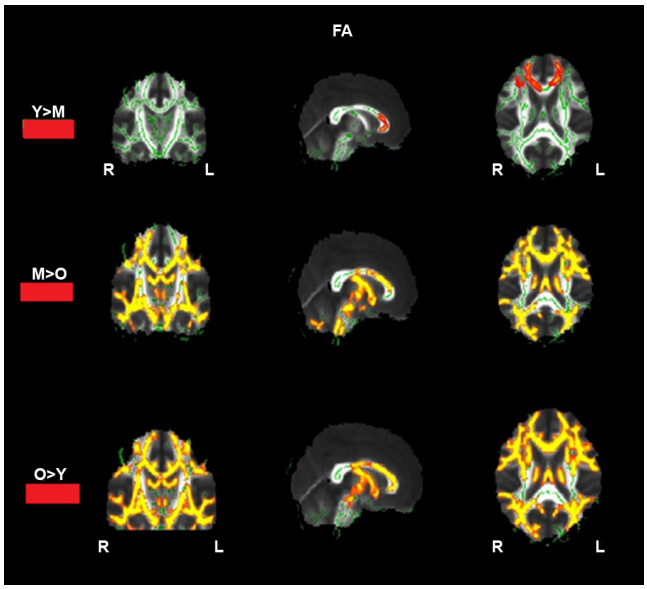

Figure 5. Statistical maps showing white matter clusters (red) where FA was significantly greater in young-aged > middle-aged adults, middle-aged > old-aged adults, old-aged > young-aged adults.
Abbreviations: FA, fractional anisotropy; R, right; L, left.

of AD and RD in old-aged group compared to young- and middle-aged groups. Similarly, we notice AD decrease in anterior/superior corona radiata, left cerebral peduncle, and retrolentricular part of internal capsule in old-aged group compared to young- and middle-aged groups and RD increase in anterior pericallosal, anterior/superior corona radiata (L), cerebral peduncle (L), and retrolentricular part of internal capsule (L) in young- and middle-aged groups compared to old-aged group.

Regression analysis between WMV and diffusion indices. Scatter plots and the results for regression analysis for WMV and diffusion indices (FA, RD, MD, and AD) using GLM are summarized in Figure 6. We noticed good correlation between global MD, AD, RD values, and WMV and poor correlation with FA in all the age groups with statistical significance $P < 0.05$.

In young adults, there was good correlation ($r = 0.7$, 0.54, and 0.65) between WMV and global MD, AD, and RD values, respectively, and $r = 0.28$ for FA. In middle-aged adults, there was good correlation ($r = 0.64$, 0.58, and 0.5) between WMV and global MD, RD, and AD values, respectively, and

Table 3. White matter clusters showing significant greater values of FA among three age groups.

WHITE MATTER LOCATION (FA)	MNI COORDINATES (CENTER OF MASS)			
	VOXELS (#)	x (mm)	y (mm)	z (mm)
Young > Middle				
Anterior corona radiata R	323	18	34	19
Anterior corona radiata L	354	–19	28	19
Genu of corpus callosum	318	15	26	19
Body of corpus callosum	346	–15	18	25
Middle > Old				
Superior corona radiata R	296	19	–17	44
Superior corona radiata L	331	–27	–17	33
Body of corpus callosum	291	9	–17	29
Fornix (column and body of fornix)	293	1	–10	16
Superior longitudinal fasciculus R	278	31	–17	38
Superior longitudinal fasciculus L	336	–31	–17	34
Anterior corona radiata R	290	18	30	–10
Anterior corona radiata L	356	–18	19	31
External capsule R	278	20	20	–10
External capsule L	299	–35	–17	–7
Posterior limb of internal capsule R	263	25	–17	17
Posterior limb of internal capsule L	293	–21	–17	1
Sagittal stratum (including inf. fronto-occipital fasciculus) R	216	42	–17	–13
Sagittal stratum (including inf. fronto-occipital fasciculus) L	299	–37	–17	–9
Fornix (cres)/stria terminalis R	226	34	–17	–11
Fornix (cres)/stria terminalis L	290	–29	–17	–10

(*Continued*)

Table 3. (*Continued*)

WHITE MATTER LOCATION (FA)	MNI COORDINATES (CENTER OF MASS)			
	VOXELS (#)	x (mm)	y (mm)	z (mm)
Cerebral peduncle R	247	19	–17	–5
Cerebral peduncle L	264	–10	–17	–17
Corticospinal peduncle R	242	7	–17	–22
Corticospinal peduncle L	255	–6	–17	–22
Middle cerebellar peduncle	251	–6	–17	–26
Old > Young				
Body of corpus callosum	289	18	–17	36
Cingulum (cingulate gyrus) R	296	9	–17	34
Cingulum (cingulate gyrus) L	314	–9	–17	34
Superior longitudinal fasciculus R	262	40	–17	32
Superior longitudinal fasciculus L	341	–34	–17	36
Posterior limb of internal capsule R	260	28	–17	17
Posterior limb of internal capsule L	297	–10	–4	3
Genus of corpus callosum	311	12	32	3
Superior corona radiata R	286	20	–19	37
Superior corona radiata L	326	–18	–17	37
Sagittal stratum (including inf. fronto-occipital fasciculus) R	221	38	–17	–12
Sagittal stratum (including inf. fronto-occipital fasciculus) L	300	–37	–13	–12
External capsule R	250	31	–17	10
External capsule L	305	–32	–18	3
Cerebral peduncle R	245	19	–17	–7
Cerebral peduncle L	271	–14	–19	–12
Fornix (cres)/stria terminalis R	289	–31	–18	–12
Fornix (cres)/stria terminalis L	226	35	–15	–12
Posterior thalamic radiation (including optic radiation) R	219	35	–42	8
Posterior thalamic radiation (including optic radiation) R	285	–39	–45	3
Retrolentricular part of internal capsule R	246	29	–21	8
Retrolentricular part of internal capsule L	299	–32	–24	3
Anterior limb of internal capsule R	282	12	3	3
Anterior limb of internal capsule L	336	–22	23	3
Anterior corona radiata R	312	17	38	3
Anterior corona radiata L	344	–24	29	3

Abbreviations: FA, fractional anisotropy; L, left; R, right.

$r = 0.38$ for FA. However, in old-aged adults, there was good correlation ($r = 0.6$, 0.58, and 0.56) between WMV and global MD, AD, and RD values, respectively, and $r = 0.3$ for FA.

Discussion

The underlying mechanism in myelination processes that lead to alterations in WM anisotropy with age is poorly understood. Till date, studies have reported changes in fiber orientation that in turn affects WM anisotropy, but they did not noticed the association of WM anisotropy and microstructural diffusion parameters with T1-weighted WMV.

Global changes with age. Our results are consistent with earlier studies that have shown a decline in WMV with aging.[16,33] We noticed a significant decrease in WMV as aging occurred with no significant change in young- and middle-aged groups when compared to old-aged group. The quantitative global estimates of FA, MD, AD, and RD in three age groups, namely young-, middle-, and old-aged adults, were estimated. Our results showed similar pattern of a significant increase in MD, AD, and RD values in old-aged group when compared to young- and middle-aged group and no significant change in young-aged group when compared to

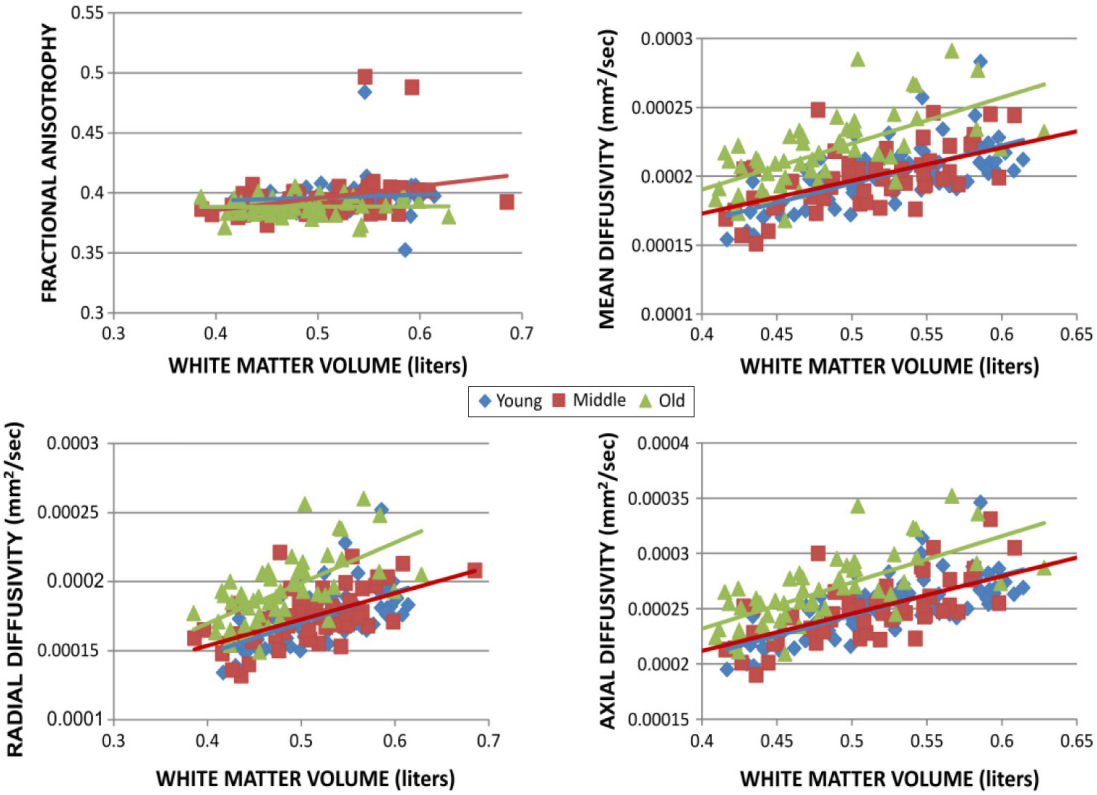

Figure 6. Scatter plots of the whole-brain values of each diffusion index vs Whole-brain white matter volume.
Abbreviations: FA, fractional anisotropy; MD, mean diffusivity; AD, axial diffusivity; RD, radial diffusivity; WMV, white matter volume.

middle-aged group. These results were consistent with earlier studies suggesting an age-related decline in the composition and integrity of WM.[34–39] On the other hand, FA showed a significant decrease in old-aged group compared to young- and middle-aged groups; however, no significant change was observed in the middle-aged group when compared to young-aged group. The decrease in FA with aging is consistent with previous studies.[22,40–42] This decline may be due to an increase in the water diffusion in the direction perpendicular to the directions of WM fibers.[43,44] This may have implications for degeneration of the myelin sheath (demyelination) and recently showed the role of apolipoprotein with WM integrity in memory decline.[45]

There are some methodological issues in group-level analysis of DTI for examining the differences in WM anisotropy development during aging process. In order to solve the important issues of cross-subject data alignment, performing localized cross-subject statistical analysis, we used TBSS. Tract-based spatial statistics method works by transforming the data from the center of the tracts that are consistent across all the subjects into a common space. Till date, studies have reported the changes of FA values in young- and middle-aged groups and young and old-aged groups.[19,23] The skeleton-wise between-group test for FA showed significantly higher FA values in young-aged group compared to middle-aged group specifically in anterior corona radiata and corpus callosum. This study reported the changes of FA values in transition from young- to middle-aged groups and middle- to old-aged groups. Analysis revealed higher FA values in middle-aged group when compared to old-aged group in 22 regions. Our analysis suggests lower FA values in older group compared to younger group in 26 WM clusters, suggesting that the integrity of WM connections degrade with age. Also, a decrease in FA is associated with a significant increase in both RD and AD,[19,46–49] and some of these changes of RD and AD are reported in earlier studies in superior corona radiata,[50] corpus callosum,[37,38] superior longitudinal fasciculus,[38,48] external capsule,[44,48,50] fornix,[48–51] sagittal striatum,[50] retrolentricular part of internal capsule,[50] and anterior/superior corona radiata.[44]

Gender differences. The gender-related effects on global WM and diffusivity measures are unclear, ie, some studies reported no gender differences[52,53] and showed a significant gender differences.[14,48,55,56] Few volumetric studies reported the life-span changes of the human brain WM.[57,58] We notice statistically significant increase in the values of WMV, FA, MD, and AD for males compared to females, which was in agreement with the previous studies.[14,20] The gender differences in FA for male subjects can be explained with three eigenvalues (λ_1, λ_2, and λ_3) analysis, which stated that these changes are due to an increase in λ_1 but no significant change in diffusion perpendicular to the fiber tract orientation (eg, λ_2 and λ_3). While analyzing within-group gender differences, we noticed a significant increase in AD values of males across

three age groups, suggesting an increase in diffusion parallel to fiber orientation rather than perpendicular direction. Within-group changes for male and female subjects were similar, ie, a gradual decline in WMV and a gradual increase in the values of MD, AD, and RD across three age groups. FA shows different pattern in males and females. In males, FA shows quadratic trajectory (inverted-U) and linear decrease in females across three age groups. Another recent study also reported that the aging effects during transition from young- to middle-aged groups were associated with more dispersion of WM fibers, while the tissue restriction and intraaxonal volume fraction remained relatively stable.[59]

Relationship between global WM and various diffusion indices. Our findings of age-related decline in FA with age and relationship among FA and other structural indices of cerebral health are consistent with some earlier studies. It was first report utilization of FA as an index of declining WM health in normal healthy aging.[54] These reports were followed by other studies with similar findings regarding change in FA with age.[22,41] All these studies interpreted their findings of age-related decline in cerebral FA as an indication of mild demyelination and/or axonal loss. These findings may reflect the fact that even small changes with age in myelin and fiber tract density result in a higher signal change for both FA and WM density. The changes in axonal diameter and density presumably affect both WM density and anisotropy values. Hence, our special focus was to notice differences in age-related trends along with the relationship of WMV with WM integrity indices. We found good correlation between all the WM integrity indices and WMV except for FA.

Strengths and limitations of this study. The strengths of the present study is the use of the native space for each participant, which allowed us to maximize neuroanatomical validity and to avoid the misregistration, segmentation, and smoothing errors that can occur in automated or semiautomated techniques as well as other limitations of voxel-based methods that may be especially apparent in aging brains.[52,60] However, manual methods limit the choice of regions to a priori hypothesized selections, and hence, we chose TBSS. Another potentiality of this study is that we have almost significant gender sample size in all the three age groups; however, the demerits are more number of males in young-aged group and more females in old-aged groups. We found significant sex differences in FA, MD, and RD but not in AD. Furthermore, the statistical trends found in the large sample data analyses revealed few additional structure–function associations. The present study relied on data that were acquired on a single 3-T MRI scanner with TBSS implementation of the DTI analyses. However, the proposed approach will be applicable for multiple scanners, and application of new advances in DTI methods may reveal findings that were missed in earlier studies. However, the limitation of this study is the implementation of the cross-sectional data that limits to estimate and assess the age-related life-span changes and differences.

Conclusions and Future Scope

We estimated global WMV, FA, MD, AD, and RD of WM integrity in three healthy age groups. We analyzed the volumetric relationship of WMV with normal aging and also relationship of measures of WM integrity using TBSS, such as FA, MD, AD, and RD, maps with aging as well as WMV. From this study, we noticed a significant decrease in FA in four regions for middle-aged group compared to young-aged group, in 22 regions for old-aged group compared to middle-aged group, and in 26 regions for old-aged group compared to young-aged group. Another finding is the inverted-U-shaped relationship for whole-brain FA values with age and increase trend of MD, RD, and AD with aging. Also, we notice that there is a decrease in WM, FA, MD, AD, and RD in females compared to males. Thus, this study helps understand the differential relationship between microstructural integrity and WMV as the human brain undergoes normal aging and gives the reasons for this highlighting age-dependent atrophy and sheds light on the differential value of various complementary imaging techniques in the assessment of brain aging. In future, we plan to extend the findings presented here. However, the data analyses of entire dataset containing different MRI scanners at other two centers will provide more accurate information as to the nature of WM changes in life-span aging. Also, it is important to delineate the laterality differences that may play a significant role in diffusivity as aging.

Acknowledgments

We extend appreciation to the facilities of National Brain Research Centre for enabling this work.

Author Contributions

Conceived and designed the experiments: RR, VPSR, PKR. Analyzed the data: RR, VPSR. Wrote the first draft of the manuscript: RR, VPSR, PKR. Contributed to the writing of the manuscript: RR, VPSR, PKR. Agree with manuscript results and conclusions: RR, VPSR, PKR. Jointly developed the structure and arguments for the paper: RR, VPSR, PKR. Made critical revisions and approved final version: RR, VPSR, PKR. All authors reviewed and approved of the final manuscript.

REFERENCES

1. Billiet T, Madler B, D'Arco F, et al. Characterizing the microstructural basis of "unidentified bright objects" in neurofibromatosis type 1: a combined in vivo multicomponent T2 relaxation and multi-shell diffusion MRI analysis. *Neuroimage Clin*. 2014;4:649–658.
2. Billiet T, Vandenbulcke M, Madler B, et al. Age-related microstructural differences quantified using myelin water imaging and advanced diffusion MRI. *Neurobiol Aging*. 2015;36:2107–2121.
3. Giorgio A, Santelli L, Tomassini V, et al. Age-related changes in gray and white matter structure throughout adulthood. *Neuroimage*. 2010;51:943–951.
4. Raz N, Rodrigue KM. Differential aging of the brain: patterns, cognitive correlates and modifiers. *Neurosci Biobehav Rev*. 2006;30:730–748.
5. Hayakawa N, Kato H, Araki T. Age-related changes of astorocytes, oligodendrocytes and microglia in the mouse hippocampal CA1 sector. *Mech Ageing Dev*. 2007;128:311–316.
6. Ge Y, Grossman RI, Babb JS, Rabin ML, Mannon LJ, Kolson DL. Age related total gray matter and white matter changes in normal adult brain. Part I: volumetric MRI imaging analysis. *AJNR Am J Neuroradiol*. 2002;23:1327–1333.

7. Tang Y, Nyengaard JR, Pakkenberg B, Gundersen HJ. Age-induced white matter changes in the human brain: a stereological investigation. *Neurobiol Aging*. 1997;18:609–615.
8. Svennerholm L, Bostrom K, Jungbjer B, Olsson L. Membrane lipids of adult human brain: lipid composition of frontal and temporal lobe in subjects of age 20 to 100 years. *J Neurochem*. 1994;63:1802–1811.
9. Bartzokis G. Age-related myelin breakdown: a developmental model of cognitive decline and Alzheimer's disease. *Neurobiol Aging*. 2004;25(1):5–18.
10. Bartzokis G. Brain myelination in prevalent neuropsychiatric developmental disorders: primary and comorbid addiction. *Adolesc Psychiatry*. 2005;29:55–96.
11. Bartzokis G. Alzheimer's disease as homeostatic responses to age-related myelin breakdown. *Neurobiol Aging*. 2009;38(8):1341–1371.
12. Beaulieu C. The basis of anisotropic water diffusion in the nervous system—a technical review. *NMR Biomed*. 2002;15:435–455.
13. Wozniak JR, Lim KO. Advances in white matter imaging: a review of in vivo magnetic resonance methodologies and their applicability to the study of development and aging. *Neurosci Biobehav Rev*. 2006;6:762–774.
14. Hsu JL, Leemans A, Bai CH, et al. Gender differences and age-related white matter changes of the human brain: a diffusion tensor imaging study. *Neuroimage*. 2008;39:566–577.
15. Resnick SM, Goldszal AF, Davatzikos C, et al. One year age changes in MRI brain volumes in older adults. *Cereb Cortex*. 2000;10:464–472.
16. Giedd JN, Snell JW, Lange N, et al. Quantitative magnetic resonance imaging of human brain development: ages 4–18. *Cereb Cortex*. 1996;6:551–560.
17. Giedd JN, Blumenthal J, Jeffries NO. Brain development during childhood and adolescence: a longitudinal MRI study. *Nat Neurosci*. 1999;2:861–863.
18. Abe O, Yamasue H, Aoki S, et al. Aging in CNS: comparison of gray white matter volume of diffusion tensor data. *Neurobiol Aging*. 2008;29:102–116.
19. Bennett IJ, Madden DJ, Vaidya CJ, Howard DV, Howard JH Jr. Age-related differences in multiple measures of white matter integrity: a diffusion tensor imaging study of healthy aging age-related differences in multiple measures of white matter integrity: a DTI study of healthy aging. *Hum Brain Mapp*. 2010;31:378–390.
20. Inano S, Takao H, Hayashi N, Abe O, Ohtomo K. Effects of age and gender on white matter integrity. *AJNR Am J Neuroradiol*. 2011;32:2103–2109.
21. Taki Y, Thyreau B, Hashizume H, et al. Linear and curvilinear correlations of brain white matter volume, fractional anisotropy, and mean diffusivity with age using voxel-based and region-of-interest analyses in 246 healthy children. *Hum Brain Mapp*. 2013;34:1842–1856.
22. Abe O, Aoki S, Hayashi N, Yamada H, Kunimatsu A. Normal aging in the central nervous system: quantitative MR diffusion tensor analysis. *Neurobiol Aging*. 2002;23:433–441.
23. Salat DH, Tuch DS, Greve DN, et al. Age-related alterations in white matter microstructure measured by diffusion tensor imaging. *Neurobiol Aging*. 2005;26:1215–1227.
24. Salat DH, Tuch DS, Hevelone ND, et al. Age-related changes prefrontal white matter measured by diffusion tensor imaging. *Ann NY Acad Sci*. 2005;1064:37–49.
25. Zhang X, Li B, Shan B. Age-related white matter degradation rule of normal human brain: the evidence from diffusion tensor magnetic resonance imaging. *Chin Med J*. 2014;127:532–537.
26. Huang H, Fan X, Weiner M, et al. Distinctive disruption patterns of white matter tracts in Alzheimer's disease with full diffusion tensor characterization. *Neurobiol Aging*. 2012;33:2029–2045.
27. Kochunov P, Williamson DE, Lancaster J, et al. Fractional anisotropy of water diffusion in cerebral white matter across the lifespan. *Neurobiol Aging*. 2012;33:9–20.
28. Kochunov P, Glahn DC, Lancaster J, et al. Fractional anisotropy of cerebral white matter and thickness of cortical gray matter across the lifespan. *Neuroimage*. 2011;58:41–49.
29. Ashburner J, Friston KJ. Voxel-based morphometry-the methods. *Neuroimage*. 2000;11:805–821.
30. Friston KJ. Statistical parametric mapping. In: Kotter R, ed. *Neuroscience Databases: A Practical Guide*. Vol 16. Berlin: Springer; 2003:237–250.
31. Smith SM, Jenkinson M, Woolrich MW, et al. Advances in functional and structural MR image analysis and implementation as FSL. *Neuroimage*. 2004;23:208–219.
32. Smith SM, Jenkinson M, Johansen-Berg H, et al. Tract-based spatial statistics: voxelwise analysis of multi-subject diffusion data. *Neuroimage*. 2006;31:1487–1505.
33. Guttmann CRG, Jolesz FA, Kikinis R, et al. White matter changes with normal aging. *Neurology*. 1998;50(4):972–978.
34. Chen ZG, Li TQ, Hindmarsh T. Diffusion tensor trace mapping in normal adult brain using single-shot EPI technique. A methodological study of the aging brain. *Acta Radiol*. 2001;42:447–458.
35. Nusbaum AO, Tang CY, Buchsbaum MS, Wei TC, Atlas SW. Regional and global changes in cerebral diffusion with normal aging. *AJNR Am J Neuroradiol*. 2001;22:136–142.
36. Rovaris M, Iannucci G, Cercignani M, et al. Age-related changes in conventional, magnetization transfer, and diffusion-tensor MR imaging findings: study with whole-brain tissue histogram analysis. *Radiology*. 2003;227:731–738.
37. Sullivan EV, Adalsteinsson E, Pfefferbaum A. Selective age-related degradation of anterior callosal fiber bundles quantified in vivo with fiber tracking. *Cereb Cortex*. 2006;16:1030–1039.
38. Madden DJ, Spaniol J, Costello MC, et al. Cerebral white matter integrity mediates adult age differences in cognitive performance. *J Cogn Neurosci*. 2009;21:289–302.
39. Peters A. The effects of normal aging on myelin and nerve fibers: a review. *J Neurocytol*. 2002;31:581–593.
40. Moseley M. Diffusion tensor imaging and aging- a review. *NMR Biomed*. 2002;15:553–560.
41. Sullivan EV, Pfefferbaum A. Diffusion tensor imaging in normal aging and neuropsychiatric disorders. *Eur J Radiol*. 2003;45:244–255.
42. Lehmbeck JT, Brassen S, Weber-Fahr W, Braus DF. Combining voxel-based morphometry and diffusion tensor imaging to detect age-related brain changes. *Neuroreport*. 2006;17:467–470.
43. Horsfield MA, Jones DK. Applications of diffusion-weighted and diffusion tensor MRI to white matter diseases—a review. *NMR Biomed*. 2002;15:570–577.
44. Bhagat YA, Beaulieu C. Diffusion anisotropy in subcortical white matter and cortical gray matter: changes with aging and the role of CSF-suppression. *J Magn Reson Imaging*. 2004;20:216–227.
45. Lee Y-M, Ha J-K, Park J-M, et al. Impact of apolipoprotein E4 polymorphism on the gray matter volume and the white matter integrity in subjective memory impairment without white matter hyperintensities: voxel-based morphometry and tract-based spatial statistics study under 3-tesla MRI. *J Neuroimaging*. 2016;26(1):144–149.
46. Barrick TR, Charlton RA, Clark CA, Markus HS. White matter structural decline in normal ageing: a prospective longitudinal study using tract-based spatial statistics. *Neuroimage*. 2010;51:565–577.
47. Burzynska AZ, Preuschhof C, Backman L, et al. Age-related differences in white matter microstructure: region-specific patterns of diffusivity. *Neuroimage*. 2010;49:2104–2112.
48. Sullivan EV, Rohlfing T, Pfefferbaum A. Quantitative fiber tracking of lateral and interhemispheric white matter systems in normal aging: relations to times performance. *Neurobiol Aging*. 2010;31:464–481.
49. Vernooij MW, Groot MD, van der Lugt A, et al. White matter atrophy and lesion formation explain the loss of structural integrity of white matter in aging. *Neuroimage*. 2008;43:470–477.
50. Burzynska A, Nagel IE, Preuschhof C, et al. Cortical thickness is linked to executive functioning in adulthood and aging. *Hum Brain Mapp*. 2012;33:1607–1620.
51. Zahr NM, Rohlfing T, Pfefferbaum A, Sullivan EV. Problem solving, working memory, and motor correlates of association and commissural fiber bundles in normal aging: a quantitative fiber tracking study. *Neuroimage*. 2009;44:1050–1062.
52. Kennedy KM, Erickson KI, Rodrigue KM, et al. Age-related differences in regional brain volumes: a comparison of optimized voxel-based morphometry to manual volumetry. *Neurobiol Aging*. 2009;30:1657–1676.
53. Ota M, Obata T, Akine Y, et al. Age-related degeneration of corpus callosum measured with diffusion tensor imaging. *Neuroimage*. 2006;31:1445–1452.
54. Sullivan EV, Adalsteinsson E, Hedehus M, et al. Equivalent disruption of regional white matter microstructure in ageing healthy men and women. *Neuroreport*. 2001;12:99–104.
55. Huster RJ, Westerhausen R, Kreuder F, Schweiger I, Wittling W. Hemispheric and gender related differences in the midcingulum bundle: a DTI study. *Hum Brain Mapp*. 2009;30:383–391.
56. Oh JS, Song IC, Lee JS, et al. Tractography-guided statistics (TGIS) in diffusion tensor imaging for the detection of gender difference of fiber integrity in the midsagittal and parasagittal corpora callosa. *Neuroimage*. 2007;36:606–616.
57. Westlye LT, Walhovd KB, Dale AM, et al. Life-span changes of the human brain white matter: diffusion tensor imaging (DTI) and volumetry. *Cereb Cortex*. 2010;20(9):2055–2068.
58. Walhovd KB, Westlye LT, Amlien I, et al. Consistent neuroanatomical age-related volume differences across multiple samples. *Neurobiol Aging*. 2011;32(5):916–932.
59. Kodiweera C, Alexander AL, Harezlak J, McAllister TW, Wu Y-C. Age effects and sex differences in human brain white matter of young to middle-aged adults: a DTI, NODDI, and q-space study. *Neuroimage*. 2016;128:182–192.
60. Sullivan EV, Pfefferbaum A. Diffusion tensor imaging and aging. *Neurosci Biobehav Rev*. 2006;30:749–761.